JMEPEG (2022) 16:7302–7314
https://doi.org/10.1007/s11665-022-06751-2

1059-9495/$19.00

TECHNICAL ARTICLE

Sustainable Hard Machining of AISI 304 Stainless Steel Through TiAlN, AlTiN, and TiAlSiN Coating and Multi-Criteria Decision Making Using Grey Fuzzy Coupled Taguchi Method

C. Moganapriya, R. Rajasekar, R. Santhosh, S. Saran, S. Santhosh, V.K. Gobinath, and P.Sathish Kumar1

Submitted: 17 August 2021 / Revised: 15 February 2022 / Accepted: 18 February 2022 / Published online: 14 March 2022

High strength, high ductility, low thermal conductivity and high work hardening effects of austenitic stainless steels are the foremost factors that make their machinability difficult. Machining, especially dry machining of such steels, has been one of the most significant challenges for carbide cutting tools. In this research study, TiAlN, AlTiN and TiAlSiN coatings were successfully employed through HiPIMS coating system on cutting tools for dry machining of AISI 304 stainless steel. As-deposited coatings were confirmed through FESEM and XRD analysis. The input process parameters including coating material have been considered for optimizing the multiple objectives such as surface roughness Ra, Rz, tool wear rate and material removal rate. Multi-criteria decision making involving grey fuzzy coupled Taguchi method was adopted to solve the optimization for multiple response characteristics. Analysis of variance was conducted to analyze the contribution percentage of each process parameter. From the results of MCDM-based GFCT, the optimized setting for best output responses was determined as coating: TiAlSiN, cutting speed: 180 m/min, feed rate: 0.1mm/rev and depth of cut: 1.5 mm. Feed rate had significantly contributed about 42.74% on the output measures, followed by coating, depth of cut and cutting speed. The responses were predicted with an accuracy of 96.5% through GFCT technique. Finally, a confirmatory experiment was carried out to support the accuracy of optimal process parameters.

Keywords AISI 304 steel, coating, fuzzy, grey, taguchi

1. Introduction

Among different steel grades, AISI 304 grade holds excellent corrosion resistance and hence employed in wide variety of applications such as vaporizer coils, kitchen sinks, food handling units, chemical processing units, automotive exhausts, cooking pans, pressure vessels and mining materials handling equipment. Machining of AISI 304 stainless steel is quite tedious process, due to its high strength and higher work hardening rate. This might lead to shorter tool life, high tool wear, higher machining time and machining cost. The tool life phenomenon and unpredictable cutting forces have direct impact on overall machining cost and dimensional accuracy of machined work piece. Several attempts were carried out in reducing the cutting forces with the view of achieving better machinability (Ref 1, 2).

Super hard thin-film surface coating on cutting tool inserts makes them more resistant to abrasion and oxidation. These coatings also act as solid lubricant at the tool–workpiece interface, which led to a decrease in temperature at cutting

Abbreviations	
WC	Tungsten carbide
ANOVA	Analysis of variance
DoE	Design of experiments
FESEM	Field emission scanning electron microscope
HiPIMS	High-power impulse magnetron sputtering
MRR	Material removal rate
S/N	Signal-to-noise ratio
SEM	Scanning electron microscope
SR	Surface roughness
TW	Tool wear
XRD	X-ray diffraction analysis
MCDM	Multi-criteria decision making
GRA	Grey relational analysis
GRG	Grey relational grade
GFRG	Grey fuzzy relational grade
GFCT	Grey fuzzy coupled Taguchi

C. Moganapriya and **P.Sathish Kumar**, Department of Mining Engineering, Indian Institute of Technology Kharagpur, Kharagpur, West Bengal, India; **R. Rajasekar, R. Santhosh, S. Saran,** and **S. Santhosh**, Department of Mechanical Engineering, Kongu Engineering College, Erode, Tamil Nadu, India; **V.K. Gobinath**, Department of Mechatronics Engineering, Kongu Engineering College, Erode, Tamil Nadu, India. Contact e-„mail: rajasekar.cr@gmail.com.

zone. Various materials were utilized as coating material for cutting tool inserts, among them titanium aluminum nitride-coated tool inserts exhibit better machinability than titanium nitride-coated tools (Ref 3-5). These surface coatings indirectly improve the working life of tool and reduce tool wear especially at increased machining speed (Ref 4, 6). As compared to single- and double-layer surface films, multilayer films experience enhanced hardness and reduce the possibility of tool failure (Ref 5, 7-10).

The machining parameters such as feed rate, cutting speed and depth of cut also influence the degree of machining in addition to surface coatings of tool insert. However, further optimizing the machining parameters will surely increase the tool life and quality of machining (Ref 11-18). It was indicated that cutting speed has greatest influence on cutting force, cutting temperature and tool life but feed rate has a significant influence on surface roughness. Furthermore, titanium oxide was present on the worn surface, which helps to increase the hardness of cutting zone, lower the friction coefficient and act as an insulator. As a result, the wear rate is reduced (Ref 10, 19). The machining parameters were optimized in turning of AISI 316L steel for attaining maximum material removal rate and surface roughness (Ref 20). For optimizing tool wear, cutting pressure, surface roughness and material removal rate, Taguchi technique and grey relational analysis were found to be more effective (Ref 21). Adoptive modeling was implemented for the prediction and validation of input to output relation with experimental outputs during turning of AISI 202L steel (Ref 22). The multi-response optimization of parameters was performed with the combined effect of Taguchi, regression analysis, response surface methodology and grey relational analysis (Ref 23-25). The optimal machining parameters on wet machining of F55 steel were achieved through Taguchi-grey relational analysis (Ref 26).

During machining of AISI 304 steel, the influence of cutting velocity on various output parameters such as tool wear and surface roughness was premeditated (Ref 27). The effect of various coolants during machining of AISI 304 steel on cutting tool performance was examined by Xavior (Ref 28). A technique of sound processing was incorporated in evaluating the optimized machining parameters such as surface roughness, formation of chip, built-up-edge formation and flank wear (Ref 29). Through design of experiments, the most reliable technique for optimizing various engineering problems is found to be Taguchi method (Ref 18, 30, 31). Design of experiments was most helpful in recognizing and optimizing machining parameters and predicting optimal combinations (Ref 32-35). Multi-output response optimization can be easily carried out with various techniques such as grey relational analysis, data evaluation and ranking, genetic algorithm, response surface methodology and artificial neural network (Ref 1, 9, 36-38).

Optimizing multiple output parameters with the view of attaining maximum performance was evaluated through various advance optimization tools such as artificial intelligence, grey relational analysis and fuzzy logic. The fuzzy logic might be helpful in addressing the indefinite and uncertain experimental values (Ref 39). For achieving effective weldability, fuzzy logic approach was applied for obtaining optimal welding parameters (Ref 40). Application of fuzzy logic approach with the grey relational analysis shall enhance degree of machining parameter optimization with the view of surpassing multi-response issues (Ref 41). Many research works were carried out in elevating the cutting tool performance through surface engineering of tool inserts. From various studies, it is evident that turning parameter optimization and input parameter influence over output machining responses were extensively explored. In addition to this, certain optimization techniques are found to be more effective in determining the optimal solution of both single and multi-response problems such as Taguchi technique, fuzzy logic and grey relational analysis (Ref 1, 32, 33, 37, 41-43).

Although numerous optimization tools are used to optimize manufacturing process parameters, there is still a high expectation of a simplified and more efficient multi-criteria decision making methodology (MCDM). The grey fuzzy technique in connection with the same method has shown itself to be efficient for the simplest methodology and similar results in accordance with the output values derived from other optimization tools. Several researchers used this approach to optimize various machining operations. Since the use of grey fuzzy-based Taguchi technique to optimize machining parameters during dry machining of AISI 304 steel was unexplored, this research study addresses the research gap by studying the same by employing the coated TiAlN, AlTiN and TiAlSiN tungsten carbide (WC) inserts. Moreover, the research study also extended in employing a simplified optimizing tool, namely grey fuzzy coupled Taguchi technique, for achieving appropriate machining process parameters in an efficient manner. The aim and objective of the research work is to deposit hard TiAlN, AlTiN and TiAlSiN coating on cutting tool insert and to perform multi-criteria decision making for identifying best optimal parameters in dry turning AISI 304 steel through grey fuzzy coupled Taguchi technique.

2. Experimental Detail and Methodology

2.1 Hard Coating on Cutting Tool

In this research study, uncoated tungsten carbide CNC cutting tool inserts were procured from Usman Tools, Coimbatore, Tamil Nadu. The insert is in the form of 4 cm diamond bar and width of the cutting-edge is 12 mm. The negative rake angle inserts have 8 mm nose radius (80° diamond sized insert) and conform to ISO CNMG 120408 standard geometrically. The hardness of uncoated insert was found to be 19.1 GPa.

Thin-film TiAlN, AlTiN, and TiAlSiN coatings were adhered to the surfaces of uncoated tungsten carbide turning tool inserts using commercially available high-power impulse magnetron sputtering system (HiPIMS) at Famex Coating India Pvt. Ltd., Coimbatore, Tamil Nadu, as shown in Fig. 1. The sputtering targets such as TiAl, AlTi, and TiAlSi were procured from Sigma-Aldrich (99.99% purity). The operating conditions for the coating deposition are listed in Table 1. The deposition was carried out in a hybrid deposition setup at a base pressure of 2 x 10^{-3} Pa (Ref 44). The operational parameters for deposition such as bias voltage, pressure and supply voltage were set to 400 V, 0.8 Pa and 950 V, respectively.

To ensure high level of cleanliness, all uncoated inserts were manually polished and ultrasonically cleaned prior to deposition. The substrates were cleansed for another 30 minutes using glow discharge at 1000 V substrate bias voltage and 1.5 Pa argon pressure. The high purity argon and nitrogen gas (99.99 percent) were utilized, and the temperature for deposition was regulated at 510 °C. The deposition chamber comprises 99.99% pure TiAl (Ti: 0.60 Al: 0.40), AlTi (Ti: 0.40, Al: 0.60) and TiAlSi targets (Ti: 0.64, Al: 0.3, Si: 0.06), which are mounted on the internal walls of deposition chamber in rectangular form.

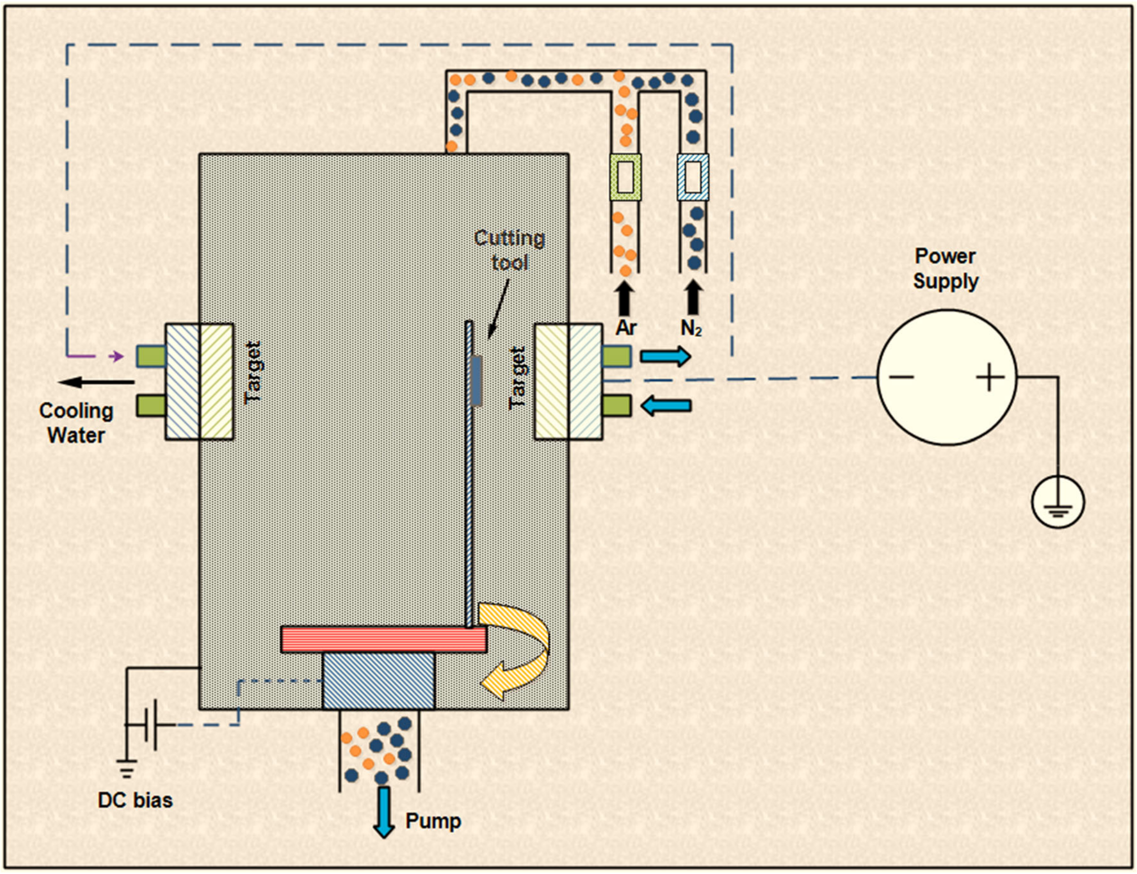

Fig. 1 Schematic diagram of HiPIMS coating process

Table 1 HiPIMS deposition parameter

Parameters	Base pressure	Pulse width	Frequency	Bias voltage	Supply voltage	Pressure
Setting	2 x 10^{-3} Pa	200 µs	50 Hz	400 V	950 V	0.8 Pa

In HiPIMS coating technique, nitrogen was used as reactive gas, which has the flow rate of approximately 94 sccm. Nitrogen ion implantation was exploited to strengthen adhesion between coating and substrate before deposition. The substrate holder was continuously rotated through the stepper motor between the sputtering targets. The substrates were rotated three cycles to aid in the uniform distribution of depositing flux throughout the surface of substrates. Thin-film TiAlN, AlTiN, and TiAlSiN layers were sputter-coated on cutting tool inserts by employing the process parameters as listed in Table 1 (Ref 45). The photographic images of coated tools are shown in Fig. 2. The coated inserts were firmly fixed to ISO PCLNR 2525 M12 assigned tool holder for Jobber XL CNC turning center as shown in Fig. 3.

Fig. 2 Images of coated tools

2.2 Characterization of Coated Inserts

The coated tools were sectionally divided into two halves by wire cutting EDM machine to measure the thickness of coating. In addition to sample cleaning and assembly, coated tools require little special preparation. When scanned through the electron beam, specimens get charged and in turn create scanning error and other picture artifacts, especially in the secondary electron imaging area. Before the analysis of FE-SEM, a thin layer of conductive gold was sputter coated to the external surface in order to evade the effects of scanning errors. By exposing the cross section through Carl Zeiss' MERLIN Field Emission Scan Electron Microscope (FE-SEM, Model: ZEISS EVO60), the thickness of coated tools was determined. X-ray diffraction (XRD, D8 Advance) with Cu K radiation

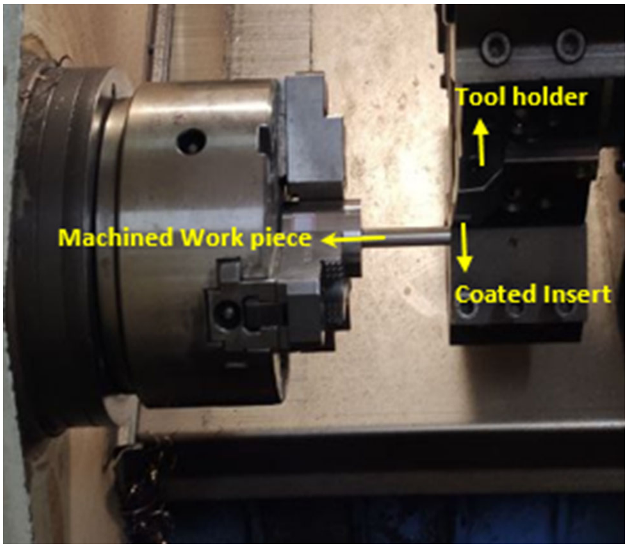

Fig. 3 Machining in CNC lathe

Table 2 AISI 304 steel—chemical composition

Element	Cr	Ni	Mn	N	S	C	Si	P
%	18	8	2	0.10	0.33	0.08	0.75	0.045

(0.15406 nm) was performed at 40 kV and 40 mA with a fixed incidence angle of 1° and scanning from 30° to 90° with a step size of 0.02°. A scratch tester was used to determine the adhesion strength between the coating and the substrate (CSM, RST). Scratch tests were performed at a maximum force of 100 N and a scratch length of 3 mm. The microhardness of TiAlN, AlTiN, and TiAlSiN coatings was measured by Vickers micro hardness tester (Wilson 400 series), which was guided by ASTM E384 Standard. The microhardness tests were carried out with an applied load 1 kg, and an indentation time of 10 s. Final microhardness result was calculated by taking average of 5 measurements on each specimen.

2.3 Workpiece

In this research work, AISI 304 SS rods of 40 mm diameter were procured from Usman Tools, Coimbatore, Tamil Nadu. The chemical composition of AISI 304 austenitic stainless steel is depicted in Table 2.

The long SS rod was cut into 9 small pieces of length 100 mm using cutting machine, and its end was faced using manual lathe as shown in Fig. 4.

2.4 Sustainable Hard Machining of AISI 304 SS

The turning experiments were carried out in dry conditions on a circular rod of AISI 304 austenitic stainless steel. As shown in Fig. 3, the experiments were carried out in computer numerical control (CNC) Lathe machine (Model: JOBBER XL). TiAlN-, AlTiN-, and TiAlSiN-coated CNC turning inserts specified in Table 3 were used. The tests were conducted three times for each cutting speed.

The experiments were designed based on the L9 orthogonal array to perform optimization study. Surface roughness (Ra and Rz), wear rate and MRR were considered as the output responses. Each experiment is performed three times, and the mean value of the output results was reported. To determine surface roughness, Mitutoyo surface tester with a travel length of 2.54 mm in the X-axis and a velocity of 0.05 cm/s was used. Wear rate was measured based on the mass difference of coated CNC tool insert before and after machining. Material removal rate was measured based on the mass difference of work piece before and after machining.

Fig. 4 AISI 304 steel work piece

Table 3 Machining data

Parameter		Levels		
Actual	Coded	Level 1	Level 2	Level 3
Coatings	A	TiAlN	AlTiN	TiAlSiN
Cutting speed, m/min	B	140	180	220
Feed rate, mm/rev	C	0.1	0.15	0.2
Depth of cut, mm	D	0.5	1.0	1.5

2.5 Multi- Criteria Decision Making-GFCT

In order to solve the simultaneous optimization of four quality characteristics such as Ra, Rz, wear rate and MRR, MCDM-based Grey fuzzy coupled Taguchi (GFCT) technique was employed. The multiple responses were first optimized by utilizing GRA (grey relational analysis) and then followed by fuzzy logic approach. Results of the fuzzy relationship grade have been optimized using S/N analysis in Taguchi single response optimization approach. The level, which has highest value for average grey fuzzy grade, is the optimum ideal condition for the output responses. ANOVA has been carried out to determine the influence and contribution by each parameter on multiple responses. Confirmation experiments were carried out to validate the optimal environment. The representation of proposed MCDM-based GFCT method is depicted in Fig. 5.

2.5.1 Grey Relational Analysis. GRA was selected to multiple such as Ra, Rz, wear rate and MRR. The optimization process in GRA constitutes three phases.

- Normalization
- Computation of grey relational coefficient
- Grey relational grade

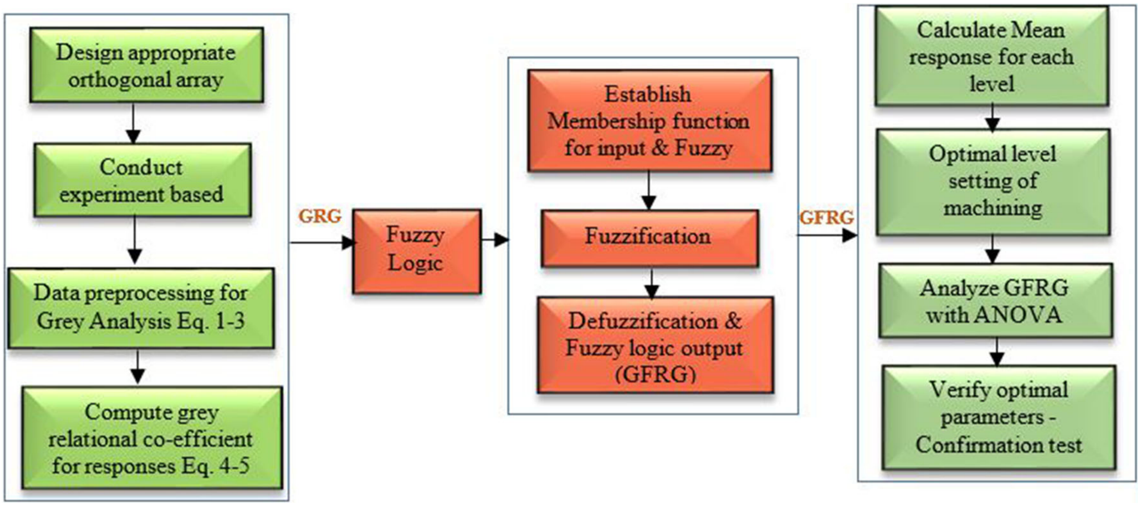

Fig. 5 Grey fuzzy coupled Taguchi method. Reprinted by permission from Springer Nature Customer Service Centre GmbH: Springer, *Structural and Multidisciplinary Optimization,* Achieving machining effectiveness for AISI 1015 structural steel through coated inserts and grey-fuzzy coupled Taguchi optimization approach, C. Moganapriya et al.,

Normalization. First step in GRA is to standardize the measured data in order to reduce difference, which is referred to data pre-processing. It is normally articulated as a range, and the unit of response varies from one individual to the next. Pre-processing of data is a better strategy for converting all original series into a relative one. The data pre-processing methods used for grey relational evaluation are as follows:

- To normalize the initial data sequence of the measured data for “higher-the-better” features (MRR), the following equation was adopted.

$$x*j = (x^\circ j(k) - \min x^\circ j(k))/(\max x^\circ j(k) - \min x^\circ j(k)) \quad \text{(Eq 1)}$$

- The “lower-the-better” features of measured data (Ra and Rz, wear rate) were normalized through the formula.

$$x*j = (\max x^\circ j(k) - x^\circ j(k))/(\max x^\circ j(k) - \min x^\circ j(k)) \quad \text{(Eq 2)}$$

- If a specific target value (preferred) is to be met, the original data set will be standardized using the following formula:

$$x*j = 1 - ((x^\circ j(k) - x^\circ j)/(\max x^\circ j(k) - x^\circ j(k))) \quad \text{(Eq 3)}$$

$x^\circ j$(k)—original set of data, x^*j(k)—next set to data pre-processing, max x^*j(k)—maximum of $x^\circ j$(k), min x^*j(k)—minimum of $x^\circ j$(k), $x^\circ j$—expected value.

Calculation of Grey Relational Coefficient. The grey contextual evaluation is used to determine the relevance of two structures. A grey relational coefficient is used to describe the sequences. It could be calculated as (k):

$$\xi(k) = (\Delta\min + \xi\Delta\max)/(\Delta\text{oj}(k) + \xi\Delta\max)) \quad \text{(Eq 4)}$$

Δoj(k)—absolute quantity of deviation from $x^\circ j$(k) and x^*j(k) (series of deviation);

ξ—coefficient of distinguishing=0.5.

The distinguished potential would be higher if the magnitude is smaller.

$$\Delta oj(k) = ||x * o(k) + x^\circ j(k)|| \quad \text{(Eq 5)}$$

Grey Relational Grade (GRG). The grey relational grade was calculated by the average of coefficients.

2.5.2 Grey Fuzzy Relational Analysis. The following four steps as part of the fuzzy rule system are shown in Fig. 5 (Ref 46).

- Fuzzification of input data
- Determination of rule base
- Decision making based on rule
- Defuzzification of data

Membership functions are established via database that are used to produce fuzzy rules. The implications of the developed rules are obtained by a decision-making unit. The fuzzy interface then turns the input into linguistic items based on their corresponding degree. The defuzzifing unit then transforms the fuzzy outputs into crisp result (Ref 46, 47). The generation of fuzzy rules is governed by if-then control principles. Table 4 portrays fuzzy technique for 2-input and 1-output system (Ref 46, 47).

Xi, Yi and Zi are fuzzy subsets that are clearly derived through their membership, for example µXi, µYi and µZi. Table 4 shows the fuzzy rule that if the inputs (A1, A2) are X1, Y1, the output B becomes Z1 and the same n number of rules can be created. The Mamdani fuzzy inference engine employs fuzzy logic technique to develop crisp results through fuzzy rules.

2.5.3 Analysis of Variance. The signal-to-noise (S/N) ratio is an efficient analysis tool for the Taguchi method to depict a quality characteristic, and higher S/N value stands for the preferred process parameter level. GFRG results were feed as single response and optimized by Taguchi method. Larger the better condition was selected for analysis grey fuzzy grade. ANOVA was used to estimate the contribution of individual parameters for selected inputs on the determined output responses. ANOVA observations could be used to determine the responsible parameters for the specified process output and can analyze parameters for best outcomes (Ref 47).

3. Results and Discussion

3.1 Characterization of Coating

The cross sections of TiAlN-, AlTiN- and TiAlSiN-coated inserts are represented in Fig. 6. The deposition of coating on cutting tool is clearly evident in the cross-sectional SEM image. From Fig. 6, coating thicknesses were measured using Image J software. The average thickness of TiAlN, AlTiN and TiAlSiN coatings is equivalent to 22.81 μm, 27.71 μm and 30.08 μm, depending on the cross section correspondingly as listed in Table 5. Figure 7 depicts the XRD patterns of deposited TiAlN, AlTiN and TiAlSiN coatings. TiAlN and AlTiN coating reveals the crystal structure of NaCl. However, there was no nitride phase observed regarding TiAlSiN coating, which is owing to the low content of Si that could replace Ti atoms in TiN lattice (FCC) and forms metastable phase of Ti(Al Si)N (Ref 48). It may also result in the formation of amorphous Si_3N_4 accumulated at the grain boundaries of nanocrystalline TiAlN (Ref 49). TiAlN and AlTiN have adhesion strengths of 45 N, 47 N, and TiAlSiN coating has a greater adhesion strength of 53 N as compared to other coatings.

Table 4 Fuzzy rules

Rule No.	Input, A1	Input, A2	Output, B
1	X1	Y1	Z1
2	X2	Y2	Z2
3	X3	Y3	Z3
n	Xn	Yn	Zn

Table 5 indicates an excellent bonding between the substrate surface and the deposited layer, thereby improving adhesive strength. This shows that physical trapping and mechanical locking have been developed and play a significant role in bonding TiAlSiN coating with tool substrate (Ref 49).

Figure 8 portrays the hardness of as-deposited TiAlN, AlTiN and TiAlSiN coatings. It was evident for Fig. 8 that TiAlSiN-coated insert possesses higher hardness of 33.67 GPa as compared to TiAlN- and AlTiN-coated inserts. The augmented

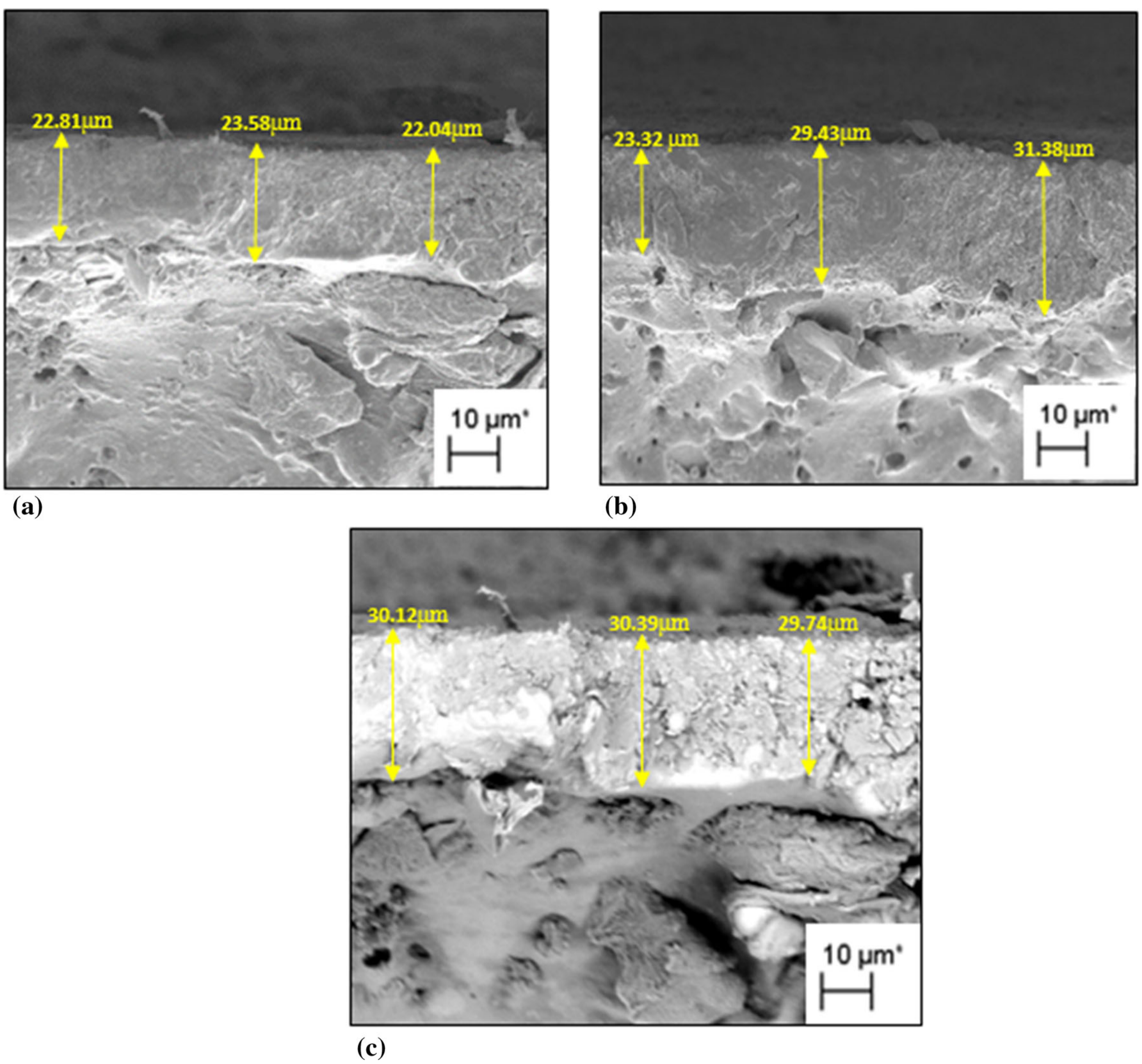

Fig. 6 Cross section FESEM image of coated tools (a) TiAlN, (b) AlTiN and (c) TiAlSiN

Table 5 Properties of deposited coating

Coating	Average Thickness, μm	Hardness, GPa	Adhesion Strength, N
TiAlN	22.81	22.21	45
AlTiN	27.71	26.15	47
TiAlSiN	30.08	33.67	53

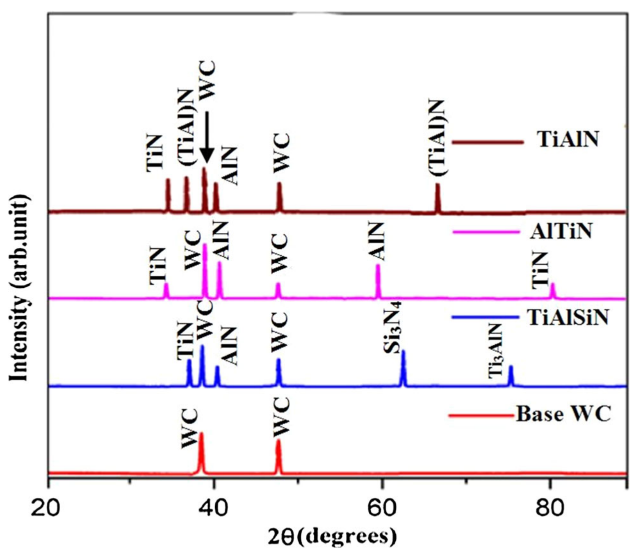

Fig. 7 XRD of base and coated inserts

hardness of TiAlSiN-coated insert could be linked with the development of nanocomposite structure consisting of nc-TiAlN embedded in a Si_3N_4 amorphous matrix that can refine grain structure (Ref 50). Furthermore, solid solution hardening can also contribute to improved hardness. The enhanced hardness of the TiAlSiN coating can be due to the combined solid solution hardening and grain boundary refinement (Ref 48).

3.2 MCDM - GFCT Method

The output responses like Ra, Rz, wear rate and MRR were measured and are listed in Table 6 based on the designed array. Each experiment was repeated three times in order to evade the inaccuracy of measurements, and the average value is reported in Table 6. In order to optimize several responses like Ra, Rz, wear rate and MRR, MCDM technique has been selected. At first, GRA has been employed in which the measured output responses (surface roughness—Ra, Rz and tool wear) were preliminary normalized using Eq 2, whereas MRR was normalized using Eq 1. Subsequently, absolute values were estimated. By substituting normalized values for all the responses in Eq 5, grey relation coefficients were obtained as listed in Table 6. The average of all the grey relational coefficients was determined, and it is termed as grey relational grade (GRG). The experiments had been ranked based on calculated GRG. From the table, experiment 8 - A3B2C1D3 (TiAlSiN, cutting speed: 180, feed rate: 0.1 and depth of cut: 1.5) attained highest rank and it was found to be the best combination of input parameters for the outputs. Moreover, the weight assignments for individual responses in GRA may result in inappropriate values. The grey fuzzy relational grade (GFRG) was subsequently implemented to mitigate these

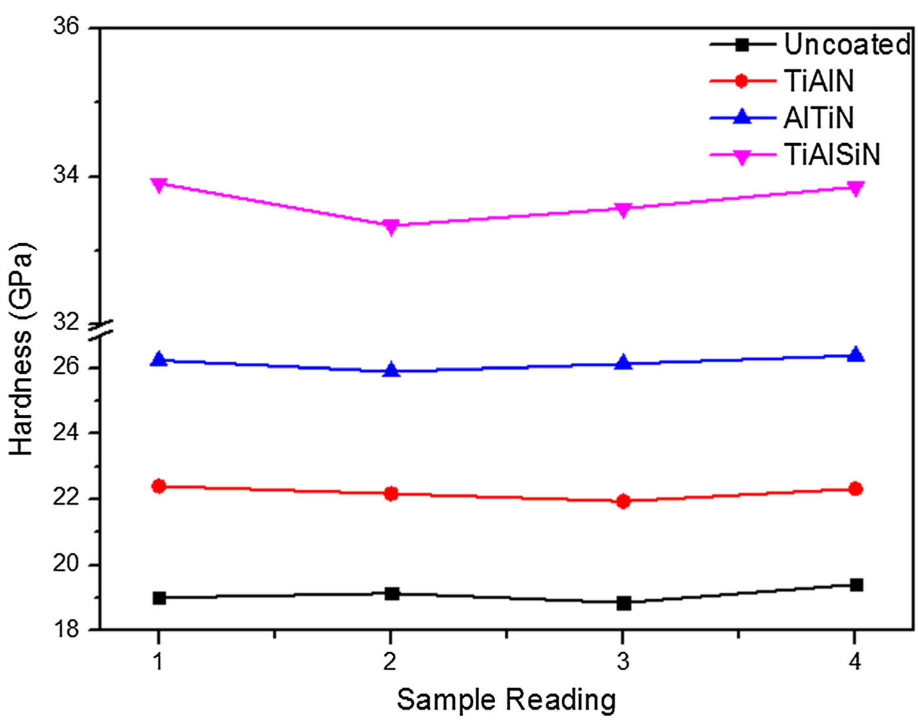

Fig. 8 Variation of hardness

Table 6 Record of experimental values and GRG

Exp. No	Coating	Cutting speed	Feed rate	Depth of cut	Ra μm	Rz μm	MRR g/s	Wear rate m^3/s	Ra Grey coefficient $\varepsilon i(k)$	Rz Grey coefficient $\varepsilon i(k)$	MRR Grey coefficient $\varepsilon i(k)$	Wear rate Grey coefficient $\varepsilon i(k)$	Grey relational grade $\varepsilon(xo, xi)$	Grey rank
1	TiAlN	140	0.1	0.5	0.4823	2.4577	1.5430	1.80E-11	0.564	0.552	0.594	0.334	0.511	6
2	TiAlN	180	0.15	1.0	0.8263	3.7413	1.5758	6.20E-12	0.361	0.381	0.612	0.640	0.498	7
3	TiAlN	220	0.2	1.5	0.9057	4.0767	1.7857	4.57E-12	0.333	0.352	0.757	0.733	0.544	4
4	AlTiN	140	0.15	1.5	0.6793	3.5777	2.0000	1.18E-11	0.427	0.396	1	0.446	0.567	3
5	AlTiN	180	0.2	0.5	0.5173	2.4547	1.0833	1.47E-11	0.534	0.552	0.422	0.385	0.473	8
6	AlTiN	220	0.1	1.0	0.3043	1.7317	1.0989	1.46E-11	0.797	0.739	0.426	0.387	0.587	2
7	TiAlSiN	140	0.2	1.0	0.7447	4.3290	0.8361	1.57E-12	0.395	0.333	0.365	1	0.523	5
8	TiAlSiN	180	0.1	1.5	0.2163	1.1757	0.6628	1.99E-12	1	1	0.333	0.952	0.821	1
9	TiAlSiN	220	0.15	0.5	0.6060	3.2177	0.8197	8.50E-12	0.469	0.436	0.362	0.543	0.452	9

consequences. The machining parameters were set as input, and GFRG was considered as output for fuzzy system as depicted in Fig. 9. Linguistic membership functions such as low, medium and high were employed to define the input variables. Also, output of the fuzzy logical system was set by averaged grey grade, and the performance of related grey grade is represented by their attributes as depicted in Table 7. In this investigation, the triangle membership function was utilized for input and output variables. A series of fuzzy guidelines were allocated based on rules as shown in Table 4.

Maximum and minimum synergistic action is generated by managing the fuzzy logic rules. In the end, the defuzzifier translates the anticipated fuzzy outputs into GFRG using fuzzy logic toolbox in MATLAB (R2016b). Table 8 encapsulates the acquired GFRG data and sample outputs from GFRG.

As described in Table 8, the optimum parameters were perceived for experiment number 8 - A3B2C1D3 (TiAlSiN, cutting speed: 180, feed rate: 0.1 and depth of cut: 1.5). The relative assessment for all GRG investigations and the accompanying GFRG is illustrated in Fig. 10. In comparison with GRG, the GFRG is enhanced by 3.53%, which reduces fuzziness. The results are consistent with the previous work (Ref 2, 51).

3.3 S/N Analysis for GFRG

The data from GFRG analysis were considered as the output response for selected process parameters, and it was optimized by Taguchi method. Since it is the most appropriate tool for optimizing single responses, augmented GFRG was optimized through Taguchi's S/N analysis.

The optimum range of process variables is the highest ratio of S/N (Ref 52). The impact of every input factor was shown more clearly in the response graph of S/N ratio. As depicted in Fig. 11, the feed rate and coating have a substantial influence on GFRG and its S/N ratios. These findings are consistent with the earlier report (Ref 33). From the S/N ratio plot, the parameter setting—A3B2C1D3 (TiAlSiN, cutting speed: 180, feed rate: 0.1 and depth of cut: 1.5)—was estimated as the best optimal parameter for GFRG and in turn for the output responses.

3.3.1 ANOVA for GFRG. The percentage contribution for GFRG was estimated, and it was observed that feed rate contributes 42.74% on the measures of GFRG as shown in Table 9. It is the most influencing parameter, which predominantly determines the value of output responses. Followed by feed rate, coating material contributes about 32.05%, whereas cutting speed and depth of cut nominally influence GFRG by 11.97 and 13.90%, respectively. From the results of S/N ratio and ANOVA, feed rate and coating have played a substantial role in enhancing the GFRG, thereby minimizing wear rate, Ra, Rz and increasing MRR. The R^2 value of ANOVA for regression of GFRG was found to be 93.47%.

It is attributed to the higher hardness of surface coating (TiAlSiN: 33.67 GPa) as illustrated in Fig. 8. The findings are in line with the Arcades rule, which stipulates that wear is exactly proportionate to the hardness of cutting tools (Ref 53). Regression equations of GFRG for TiAlN-, AlTiN-, TiAlSiN-coated inserts were determined as listed in Eq 6, 7, 8.

$$\mathrm{TiAlN}: \mathrm{GFRG} = 0.605 + 0.00012\,\text{Cutting speed} - 1.44\,\text{Feed rate} + 0.0164\ \text{Depth of cut} \quad \text{(Eq 6)}$$

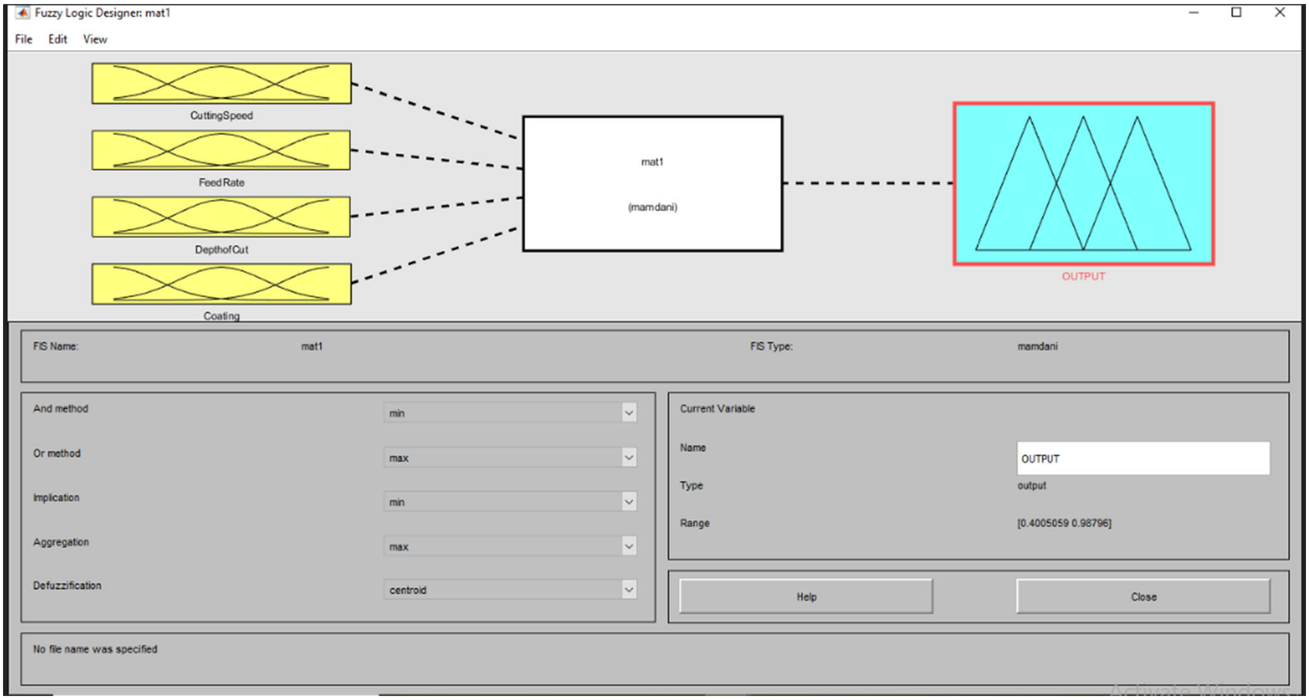

Fig. 9 GFRG system—Mamdani approach

Table 7 Intervals for sorting grade

Linguistic attributes	Lower range	Higher range
Very very small	0.452426128	0.493407686
Very Small	0.493407686	0.534389244
Small	0.534389244	0.575370802
Small medium	0.575370802	0.61635236
Medium	0.61635236	0.657333918
Medium high	0.657333918	0.698315476
High	0.698315476	0.739297034
Very high	0.739297034	0.780278592
Very very high	0.780278592	0.82126015

Table 8 Comparison of GRG and GFRG

Sl. No.	GRG	Rank	GFRG	Rank
1	0.511	6	0.541	5
2	0.498	7	0.501	8
3	0.544	4	0.551	4
4	0.567	3	0.579	3
5	0.473	8	0.509	7
6	0.587	2	0.608	2
7	0.523	5	0.531	6
8	0.821	1	0.875	1
9	0.452	9	0.464	9

$$\text{AlTiN}\ : \text{GFRG} = 0.639 + 0.00012\text{Cutting speed} - 1.44\text{Feed rate} + 0.0164\text{Depth of cut} \tag{Eq 7}$$

$$\text{TiAlSiN}\ : \text{GFRG} = 0.697 + 0.00012\text{Cutting speed} - 1.44\text{Feed rate} + 0.0164\text{Depth of cut} \tag{Eq 8}$$

Figure 12 depicts 3D surface plots of GFRG with respect to cutting speed, feed rate and depth of cut. From Fig. 12a, GFRG is higher at higher depth of cut with respect to lower and higher cutting speed. Feed rate at lower level tends to produce higher GFRG as shown in Fig. 12b. It possesses higher value at lower feed rate for low and high cutting speed. Figure 12c portrays the relation between feed rate and depth of cut with reference to GFRG. With higher depth of cut, GFRG possess higher values with respect to low and high feed rate.

3.4 Confirmation Test

An experiment on the optimum combination (A3B2C1D3) of parameters was conducted to validate the outcomes of MCDM method (TiAlSiN, cutting speed: 180, feed rate: 0.1 and depth of cut: 1.5). The results were measured and summarized as presented in Table 10.

The next step following the identification of optimal process variables is to forecast and assess the improvements in performance of optimum process parameters. Table 10 shows a comparison of several objectives with initial and optimal processing parameters. The initial level of optimal machining parameters from GFRG and GRA is A3, B2, C1 and D3, and it matches with experiment number 8 in Table 6. The optimum results were predicted, and the anticipated test results with an average error of 3.54% and an accuracy of 96.5% are validated.

These findings substantiate and validate the adopted MCDM–GFCT method. Multiple objectives have been optimized simultaneously in the turning process, and this strategy is

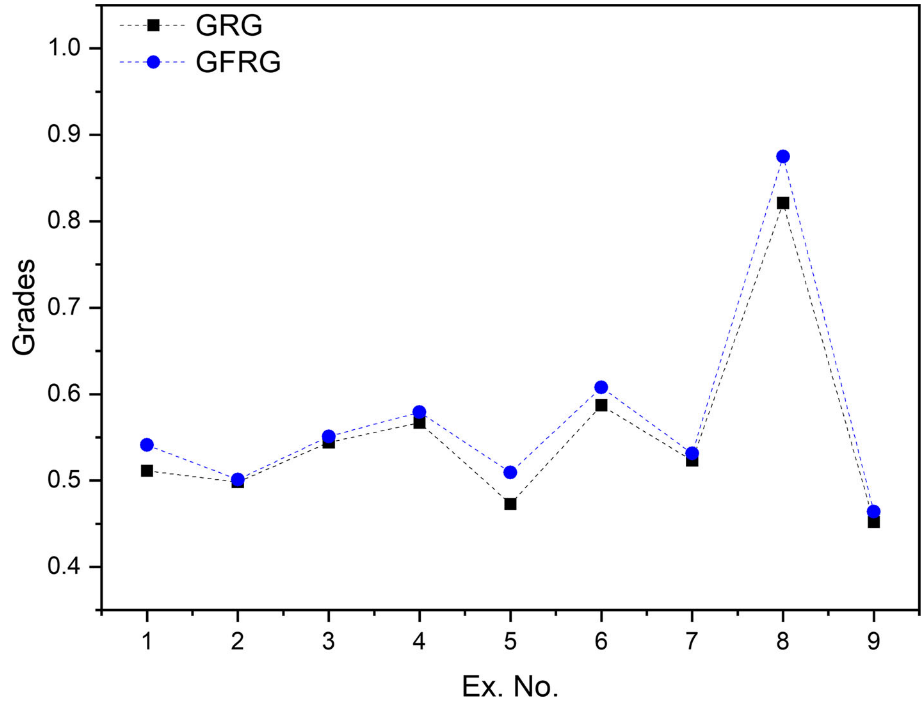

Fig. 10 Relative evaluation of GRG and GFRG

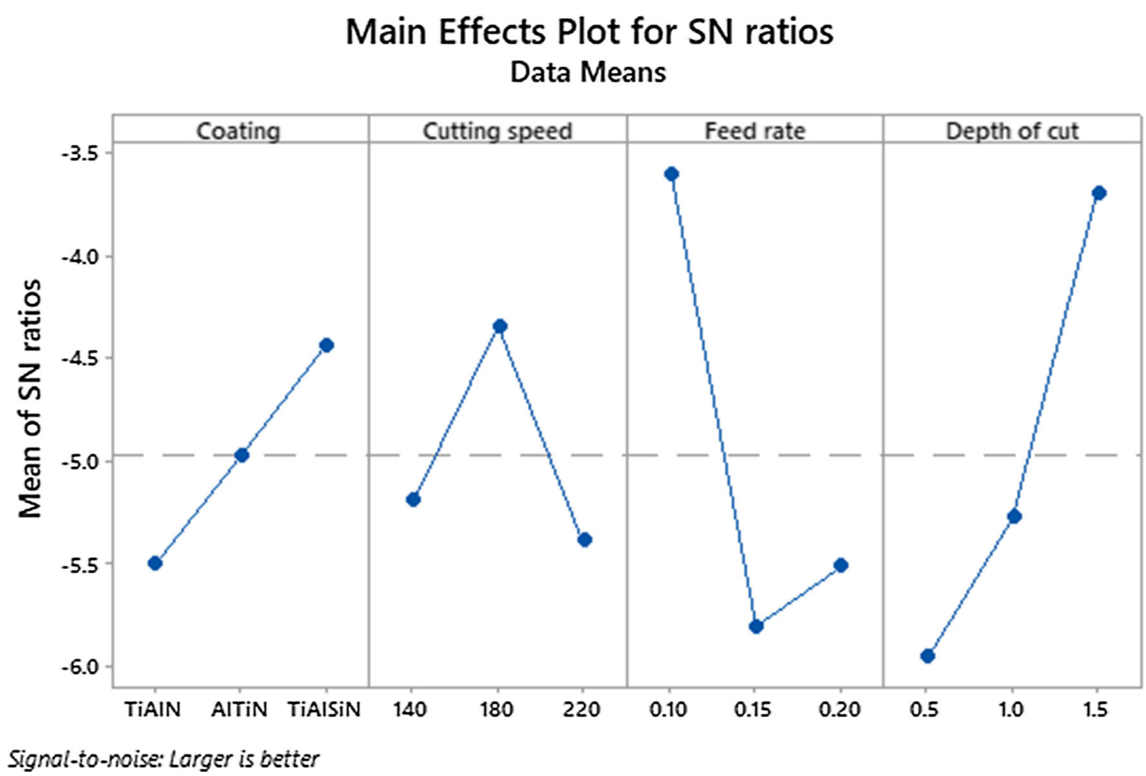

Fig. 11 Mean effects plot of S/N ratio

Table 9 Analysis of variance for regression of GFRG

Source	DF	Adj. SS	Adj. MS	*F*-Value	*p*-value	% Contribution
Regression	5	0.08463	0.01693	1.57		
Coating	1	0.03013	0.03013	2.01	0.029	32.05
Cutting speed	1	0.01125	0.01125	0.47	0.048	11.97
Feed rate	1	0.04018	0.04018	3.74	0.021	42.74
Depth of cut	2	0.01307	0.00653	0.61	0.041	13.90
Error	3	0.03227	0.01076			
Total	8	0.12689				

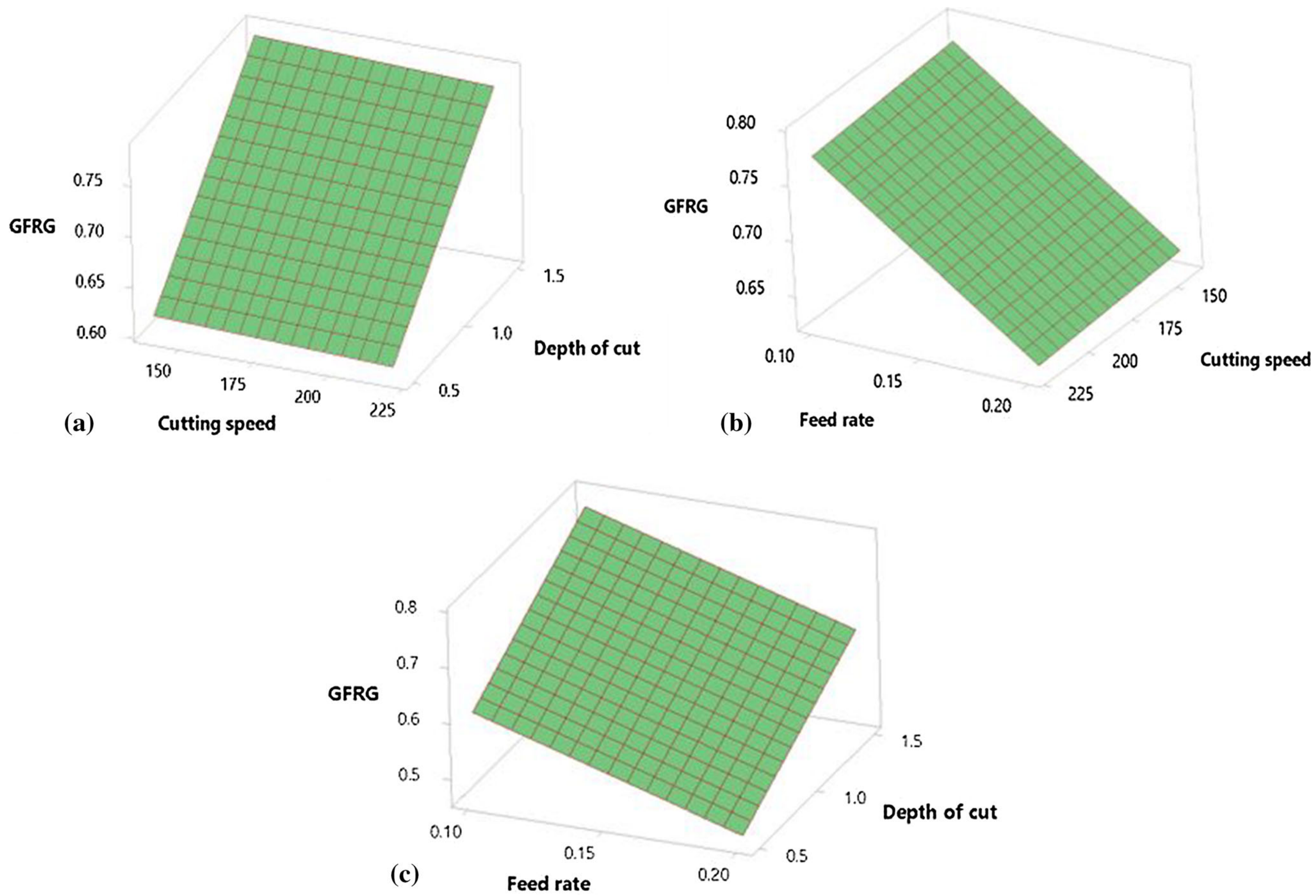

Fig. 12 3D surface plot of GFRG vs. input parameters

Table 10 Confirmation test

Initial parameters	Optimal parameters			
	Predicted value	Experimental value	Difference in values	% Error
Levels	A3B2C1D3	A3B2C1D3		
Surface roughness Ra (μm)	0.2083	0.2163	0.008	3.84
Surface roughness Rz (μm)	1.1421	1.1757	0.0336	2.94
MRR (g/s)	0.6886	0.6628	0.0258	3.75
Wear rate (m^3/s)	1.92E-12	1.99E-12	7E-14	3.65
Avg. Error				3.54
% Accuracy				96.5

clearly displayed. These results are consistent with the prior investigations (Ref 51).

4. Conclusion

Hard TiAlN, AlTiN and TiAlSiN coatings were successfully deposited on the surface of cutting tool insert through HiPIMS system. As-deposited coatings were confirmed by XRD analysis, and their coating thickness was determined by FESEM. The average thickness of TiAlN, AlTiN and TiAlSiN coatings was equivalent to 22.81, 27.71 μm and 30.08 μm. From the results of hardness measurements, TiAlSiN-coated insert exhibits higher hardness of 33.67 GPa. MCDM technique has been adopted for optimizing multiple responses like Ra, Rz, wear rate and MRR. The measured data were normalized and ranked through GRA, and the same has been fuzzified through GFRG. From ANOVA results, it was found that feed rate and coating have played a substantial role in enhancing the GFRG, thereby minimizing wear rate, Ra, Rz and increasing MRR. It contributes 42.74% on the measures of GFRG, followed by coating which contributes about 32.05%, whereas cutting speed and depth of cut nominally influence GFRG by 11.97% and 13.9%, respectively. The optimized parameters of MCDM–GFCT are TiAlSiN-coated insert, cutting speed: 180 m/min, feed rate: 0.1 mm/rev and depth of cut: 1.5 mm. The confirmation experiment has been conducted, and the results of MCDM were validated with a prediction accuracy of 96.5%. These findings confirm and substantiate the implemented MCDM–GFCT method.

References

1. S. Shankar, T. Mohanraj, and S.K. Thangarasu, Multi-Response Milling Process Optimization Using the Taguchi Method Coupled to Grey Relational Analysis, *Mater. Test.*, 2016, **58**(5), p 462–470.
2. C. Moganapriya et al., Achieving Machining Effectiveness for AISI 1015 Structural Steel Through Coated Inserts and Grey-Fuzzy Coupled Taguchi Optimization Approach, *Struct. Multidiscip. Optim.*, 2021, **63** (3), p 1169–1186.
3. D. Boing, A.J. de Oliveira, and R.B. Schroeter, Limiting Conditions for Application of PVD (TiAlN) and CVD (TiCN/Al2O3/TiN) Coated Cemented Carbide Grades in the Turning of Hardened Steels, *Wear*, 2018, **416–417**, p 54–61.
4. P.C. Jindal et al., Performance of PVD TiN, TiCN, and TiAlN Coated Cemented Carbide Tools in Turning, *Int. J. Refract Metal Hard Mater.*, 1999, **17**(1–3), p 163–170.
5. C. Moganapriya et al., Tribomechanical Behavior of TiCN/TiAlN/WC-C Multilayer Film on Cutting Tool Inserts for Machining, *Mater. Test.*, 2017, **59**(7–8), p 703–707.
6. Z. Wu et al., Electrochemical and Tribological Properties of CrAlN, TiAlN, and CrTiN Coatings in Water-Based Cutting Fluid, *J. Mater. Eng. Perform.*, 2020, **29**(4), p 2153–2163.
7. M. Kaladhar, K.V. Subbaiah, and C.S. Rao, Optimization of Surface Roughness and Tool Flank Wear in Turning of AISI 304 Austenitic Stainless Steel with CVD Coated Tool, *J. Eng. Sci. Technol.*, 2013, **8** (2), p 165–176.
8. C. Moganapriya, M. Vigneshwaran, G. Abbas, A. Ragavendran, V.H. Ragavendra, and R. Rajasekar, Technical Performance of Nano-layered CNC Cutting Tool Inserts—An Extensive Review, *Mater. Today Proc.*, 2020, **45**, p 663–669.
9. T. Sampath Kumar, S. Balasivanandha Prabu, and G. Manivasagam, Metallurgical Characteristics of TiAlN/AlCrN Coating Synthesized by the PVD Process on a Cutting Insert, *J. Mater. Eng. Perform.*, 2014, **23** (8), p 2877–2884.
10. G. Zheng et al., Effect of Cutting Parameters on Wear Behavior of Coated Tool and Surface Roughness in High-Speed Turning of 300M, *Measurement*, 2018, **125**, p 99–108.
11. N. Abburi and U. Dixit, Multi-objective Optimization of Multipass Turning Processes, *Int. J. Adv. Manuf. Technol.*, 2007, **32**(9–10), p 902–910.
12. I. Asiltürk and H. Akkuş, Determining the Effect of Cutting Parameters on Surface Roughness in Hard Turning Using the Taguchi Method, *Measurement*, 2011, **44**(9), p 1697–1704.
13. C. Nian, W. Yang, and Y. Tarng, Optimization of Turning Operations with Multiple Performance Characteristics, *J. Mater. Process. Technol.*, 1999, **95**(1–3), p 90–96.
14. B. Zou et al., Study on Microstructure and its Formation Mechanism, and Mechanical Properties of TiB2–TiC Laminated Ti(C5N5) Composite Ceramic Cutting Tool Material, *Int. J. Refract Metal Hard Mater.*, 2014, **42**, p 169–179.
15. R.Q. Sardinas, M.R. Santana, and E.A. Brindis, Genetic Algorithm-Based Multi-Objective Optimization of Cutting Parameters in Turning Processes, *Eng. Appl. Artif. Intell.*, 2006, **19**(2), p 127–133.
16. H. Zhao, G.C. Barber, and Q. Zou, A Study of Flank Wear in Orthogonal Cutting with Internal Cooling, *Wear*, 2002, **253**(9), p 957–962.
17. C. Moganapriya et al., Influence of Coating Material and Cutting Parameters on Surface Roughness and Material Removal Rate in Turning Process Using Taguchi Method, *Mater. Today Proc.*, 2018, **5** (2), p 8532–8538.
18. V.-C. Dinh, T.-P. Nguyen, and V.-C. Tong, Multi-response Optimization of 67Ni18Cr5Si4B Coating by HVOF Spray Using Taguchi-OEC Technique, *J. Adhes. Sci. Technol.*, 2019, **33**(3), p 314–327.
19. V. Sivaraman, S. Sankaran, and L. Vijayaraghavan, Effect of Cutting Parameters on Cutting Force and Surface Roughness During Machining Microalloyed Steel: Comparison Between Ferrite–Pearlite, Tempered Martensite and Ferrite–Bainite–Martensite Microstructures, *Proc. Inst. Mech. Eng. Part B J. Eng. Manuf.*, 2018, **232**(1), p 141–150.
20. Y. Touggui et al., Multi-objective Optimization of Turning Parameters for Targeting Surface Roughness and Maximizing Material Removal Rate in Dry Turning of AISI 316L with PVD-Coated Cermet Insert, *SN Appl. Sci.*, 2020, **2**(8), p 1360.
21. K. Palanikumar et al., Analysis on Drilling of Glass Fiber–Reinforced Polymer (GFRP) Composites Using Grey Relational Analysis, *Mater. Manuf. Process.*, 2012, **27**(3), p 297–305.
22. I. Shivakoti et al., ANFIS Based Prediction and Parametric Analysis during Turning Operation of Stainless Steel 202, *Mater. Manuf. Process.*, 2019, **34**(1), p 112–121.
23. A. Tamilvanan et al., Parameter Optimization of Copper Nanoparticle Synthesis by Electrodeposition Process Using RSM and CS, *Mater. Today Proc.*, 2021, **45**, p 751–756.
24. H. Kus, G. Basar, and F. Kahraman, Modeling and Optimization for Fly Ash Reinforced Bronze-Based Composite Materials Using Multi Objective Taguchi Technique and Regression Analysis, *Ind. Lubr. Tribol.*, 2018, **70**, p 1187–1192.
25. G. Başar, F. Kahraman, and G.T. Önder, Mathematical Modeling and Optimization of Milling Parameters in AA 5083 Aluminum Alloy, *Eur. Mech. Sci.*, 2019, **3**(4), p 159–163.
26. G. Dinde and G. Dhende, Study of Machining Parameters for Wet Turning of F55 Stainless Steel Using Grey Relational Analysis for Improvement in Surface Roughness, *Optimization Methods in Engineering*. Springer, Berlin, 2021, p 567–578
27. I. Korkut et al., Determination of Optimum Cutting Parameters during Machining of AISI 304 Austenitic Stainless Steel, *Mater. Des.*, 2004, **25**(4), p 303–305.
28. M. Xavior, Evaluating the Machinability of AISI 304 Stainless Steel Using Alumina Inserts, *J. Achiev. Mater. Manuf. Eng.*, 2012, **55**(2), p 841–847.
29. Z. Tekıner and S. Yeşılyurt, Investigation of the Cutting Parameters Depending on Process Sound During Turning of AISI 304 Austenitic Stainless Steel, *Mater. Des.*, 2004, **25**(6), p 507–513.
30. Y. Fedai et al., Optimization of Machining Parameters in Face Milling Using Multi-Objective Taguchi Technique, *Tehnički glasnik*, 2018, **12** (2), p 104–108.
31. G. Basar et al., Modeling and Optimization of Face Milling Process Parameters for AISI 4140 Steel, *Tehnički glasnik*, 2018, **12**(1), p 5–10.

32. C. Ahilan, S. Kumanan, and N. Sivakumaran, Application of Grey Based Taguchi Method in Multi-Response Optimization of Turning Process, *Adv. Prod. Eng. Manag.*, 2010, **5**(3), p 171–180.
33. I. Asiltürk and S. Neşeli, Multi Response Optimisation of CNC Turning Parameters via Taguchi Method-Based Response Surface Analysis, *Measurement*, 2012, **45**(4), p 785–794.
34. S.K. Khare and S. Agarwal, Optimization of Machining Parameters in Turning of AISI 4340 Steel under Cryogenic Condition using Taguchi Technique, *Procedia CIRP*, 2017, **63**, p 610–614.
35. Chinnasamy, M., et al., A Frontier Statistical Approach Towards Online Tool Condition Monitoring and Optimization for Dry Turning Operation of Sae 1015 Steel. Archives of Metallurgy & Materials, 2021. 66(3)
36. B. Das et al., Application of Grey Fuzzy Logic for the Optimization of CNC Milling Parameters for Al–4.5% Cu–TiC MMCs with Multi-Performance Characteristics, *Eng. Sci. Technol. Int. J.*, 2016, **19**(2), p 857–865.
37. S. Liu et al., Structural Optimization of the Cross-Beam of a Gantry Machine Tool Based on Grey Relational Analysis, *Struct. Multidiscip. Optim.*, 2014, **50**(2), p 297–311.
38. T. Muthuramalingam et al., Multi Criteria Decision Making of Abrasive Flow Oriented Process Parameters in Abrasive Water Jet Machining Using Taguchi–DEAR Methodology, *SILICON*, 2018, **10** (5), p 2015–2021.
39. Başar, G. and F. Kahraman, Prediction Of Surface Hardness in a Burnishing Process Using Taguchi Methot, Fuzzy Logic Model and Regression Analysis. 2018
40. P. Sathiya et al., Optimization of Laser Butt Welding Parameters Based on the Orthogonal Array with Fuzzy Logic and Desirability Approach, *Struct. Multidiscip. Optim.*, 2011, **44**(4), p 499–515.
41. Zadeh, L.A., G.J. Klir, and B. Yuan, Fuzzy sets, fuzzy logic, and fuzzy systems: selected papers. Vol. 6. 1996: World Scientific
42. Huu Phan, N. and T. Muthuramalingam, Multi Criteria Decision Making of Vibration Assisted EDM Process Parameters on Machining Silicon Steel Using Taguchi-DEAR Methodology. Silicon, 2020
43. Moganapriya, C., et al., Dry Machining Performance Studies on TiAlSiN Coated Inserts in Turning of AISI 420 Martensitic Stainless Steel and Multi-Criteria Decision Making Using Taguchi-DEAR Approach. Silicon, 2021: pp. 1–14
44. G. Li et al., The Performance of TiAlSiN Coated Cemented Carbide Tools Enhanced by Inserting Ti Interlayers, *Metals*, 2019, **9**(9), p 918.
45. H. Pekşen and A. Kalyon, Optimization and Measurement of Flank Wear and Surface Roughness Via Taguchi Based Grey Relational Analysis, *Mater. Manuf. Process.*, 2021, **36**, p 1–10.
46. Klir, G. and B. Yuan, Fuzzy sets and fuzzy logic. Vol. 4. 1995: Prentice hall New Jersey
47. N. Senthilkumar, J. Sudha, and V. Muthukumar, A Grey-Fuzzy Approach for Optimizing Machining Parameters and the Approach Angle in Turning AISI 1045 Steel, *Adv. Prod. Eng. Manag.*, 2015, **10** (4), p 195–208.
48. D. Yu et al., Microstructure and Properties of TiAlSiN Coatings Prepared by Hybrid PVD Technology, *Thin Solid Films*, 2009, **517**(17), p 4950–4955.
49. J. Liu et al., Cutting Performance and Wear Behavior of AlTiN- and TiAlSiN-Coated Carbide Tools During Dry Milling of Ti–6Al–4V, *Acta Metallurgica Sinica (Engl. Lett.)*, 2020, **33**(3), p 459–470.
50. O. Durand-Drouhin et al., Mechanical Properties and Failure Modes of TiAl (Si) N Single and Multilayer Thin Films, *Surf. Coat. Technol.*, 2003, **163**, p 260–266.
51. C. Ahilan, S. Kumanan, and N. Sivakumaran, Multi-objective Optimisation of CNC Turning Process Using Grey Based Fuzzy Logic, *Int. J. Mach. Mach. Mater.*, 2009, **5**(4), p 434–451.
52. J.T. Krishankant, M. Bector, and R. Kumar, Application of Taguchi Method for Optimizing Turning Process by the Effects of Machining Parameters, *Int. J. Eng. Adv. Technol.*, 2012, **2**(1), p 263–274.
53. M.E. Abdelmoneim, and R. Scrutton, The Tribology of Cutting Tools During Finish Machining. I, *Wear*, 1973, **25**(1), p 45–53.